Supporting Information

Lu et al. 10.1073/pnas.1308936110

SI Materials and Methods

Plant Materials. Samples were collected from 6-mo-old *Populus trichocarpa* (Nisqually-1) WT and transgenic trees maintained in a greenhouse as described (1).

***PtrLAC* Gene Identification and Phylogenetic Analysis.** *PtrLACs* were identified by comparison of 17 *Arabidopsis* laccase protein sequences (TAIR, www.arabidopsis.org/) against the *P. trichocarpa* genome v2.2 using the tBLASTn and BLASTp algorithms (www.ncbi.nlm.nih.gov/BLAST) (2, 3), applying an e-value cutoff of $1e^{-10}$ to screen for functional homologs (4, 5). Cu-oxidase domains were detected by BLAST of the deduced PtrLAC sequences against the National Center for Biotechnology Information conserved domain database (www.ncbi.nlm.nih.gov/Structure/cdd/wrpsb.cgi). A phylogenetic tree was constructed using MEGA 5.1 (6). The reliability of branching was assessed by bootstrap resampling using 1,000 replicates. Nodes supported by bootstrap probabilities >50% are shown.

Quantitative Real-Time PCR of Laccase Transcript Abundance. Total RNAs from young leaves, mature leaves, young stems, young roots, stem differentiating xylem (SDX), and phloem were isolated using cetyltrimethylammonium bromide (CTAB) (7). Gene-specific forward and reverse primers (Table S6) were used for quantitative RT-PCR (qRT-PCR) to estimate gene-specific laccase transcript abundance in different tissues as described (8, 9).

Computational Prediction and Experimental Validation of ptr-miR397a Targets. Ptr-miR397a targets were predicted from the *P. trichocarpa* genome v2.2 by the psRNATarget server (2, 10). A penalty score cutoff of 2.5 calculated as previously described (11) was applied to potential target sites in the microRNA (miRNA): mRNA duplexes. Experimental validation of predicted targets was carried out using a modified RNA ligase-mediated 5′-rapid amplification of cDNA ends (RACE) using the GeneRacer kit (Invitrogen) as described (11). PCRs were performed on cDNA from SDX and young roots of 6-mo-old *P. trichocarpa* plants using the GeneRacer 5′ primer and gene-specific primers (Table S7). Nested PCRs were performed using the GeneRacer 5′ nested primer and the nested gene-specific primers (Table S7).

Isolation of *PtrMIR397a* cDNA. The transcriptional start site and the polyadenylation site of *PtrMIR397a* were determined by 5′- and 3′-RACE using GeneRacer. The gene-specific and nested gene-specific primers are 5′-GTGAGCTCCACAGACCACGCAAAT-3′ and 5′-CGCAAATGCCTGTTTCGCACCACAA-3′ for 5′ RACE and 5′-GCATCTTGAAGCATTGGAATCAGAGA-3′ and 5′-CAGAGATACGAGGGCCCAATGGTA-3′ for 3′ RACE, respectively. The *PtrMIR397a* cDNA was amplified by PCR using the gene-specific forward primer (5′-GCGGATCCATTGCA-TTTGAAAGTGAGCTAGCTA-3′; BamHI site is underlined) and the gene-specific reverse primer (5′-GTCCCGGGCTTAG-AACTTACACGGGACCTA-3′; SmaI site is underlined). PCR products were cloned into *pCR4-TOPO* vectors (Invitrogen) and sequence validated.

Vector Construction of CaMV35Sp::*MIR397a* and Transformation. The *PtrMIR397a* cDNA was excised from the *pCR4-TOPO* vector with BamHI/SmaI and then inserted into the modified *pBI121* with a double CaMV 35S promoter to replace the *GUS* gene. The construct was mobilized into *Agrobacterium* strain C58 using the freeze/thaw method for *P. trichocarpa* transformation as described (12).

Light Microscopy. The stem transverse section preparation and image taken were followed as described by Li et al. (1).

qRT-PCR Analysis of Ptr-miR397a. SDX total RNA from three WT trees and nine transgenic lines of overexpressing *PtrMIR397a* was isolated using CTAB (7). Quantitation of ptr-miR397a by qRT-PCR was conducted as described (13).

Wood Chemical Composition. Debarked increment cores (12 cm) were cut into two sections (6 cm), placed in acetone, and held for 2 d at room temperature. Acetone was drained and replaced four times at 48-h intervals. After drying, the wood was ground in a Wiley mill with a 40-mesh screen. The resulting wood meals (40–60 mesh) was used for lignin content determination (14) to estimate both Klason lignin and acid-soluble lignin for total lignin content using an extinction coefficient of 110 $g^{-1}\cdot cm^{-1}$ at 205 nm (15). Neutral sugars in the acid-soluble fraction were derivatized to alditol acetates for quantitation by gas chromatography using a flame ionization detector (GC-FID; Agilent 7890A) (16). The uronic acid content was determined by the sulfuric acid-carbazole method (17). Glucuronolactone was used as the standard, and the optical density was measured at 530 nm.

Nitrobenzene Oxidation Analysis. Nitrobenzene oxidation analysis was conducted following Katahira and Nakatsubo (18). Extractive-free wood meal was oxidized with nitrobenzene, extracted with CH_2Cl_2, trimethylsilylated with *N*-methyl-*N*-(trimethylsily1)-trifluoroacetamide (Sigma), and quantified by GC-FID using a DB-5 GC-column.

NMR Sample Preparation and NMR Experiments. Two grams of 40- to 60-mesh wood meal samples were ball-milled using a Planetary micromill Pulverisette 7 (Fritsch, Germany) in a 50-mL ZrO_2 bowl with 18 ZrO_2 ball bearings (1 cm diameter) at 600 rpm, with 15 min of rest after every 30 min of milling. The total actual milling time for each sample was 3 h. Cellulolytic enzyme lignin (CEL) was isolated according to Chang et al. (19). One gram of the ball-milled material was suspended in 20 mL 20 mM NaOAc buffer (pH 4.5). Crude cellulase (50 mg) was added, and the reaction was incubated at 48 °C for 48 h. The solution was centrifuged, and the residues were washed with 20 mL distilled water three times and freeze-dried.

The CELs were collected directly into NMR tubes (40 mg for each sample) and dissolved using DMSO-d_6/pyridine-d_5 (4:1) (20, 21). NMR spectra were acquired on a Bruker Biospin Avance 700-MHz spectrometer equipped with a cryogenically cooled 5-mm TXI $^1H/^{13}C/^{15}N$ gradient probe with inverse geometry (proton coils closest to the sample). The central DMSO solvent peak was used as an internal reference (δ_C, 39.5; δ_H, 2.49 ppm). The ^{13}C–^1H correlation experiment was an adiabatic heteronuclear single-quantum correlation (HSQC) experiment (Bruker standard pulse sequence "hsqcetgpsisp.2"; phase-sensitive gradient-edited-2D HSQC using adiabatic pulses for inversion and refocusing) (22). HSQC experiments were carried out using the following parameters: acquired from 11.5 to −0.5 ppm in F2 (^1H) with 3,366 data points (acquisition time, 200 ms) and 215 to −5 ppm in F1 (^{13}C) with 560 increments (F1 acquisition time, 7.2 ms) of 32 scans with a 1-s interscan delay; the d_{24} delay was set to 0.86 ms (1/8J, J = 145 Hz). The total acquisition time for a sample was 6 h. Processing used typical matched Gaussian apodization (GB = 0.001, LB = −0.5) in F2 and squared cosine-

bell and one level of linear prediction (32 coefficients) in F1. Volume integration of contours in HSQC plots used Bruker's TopSpin 3 (Mac version) software and used spectra reprocessed without linear prediction.

RNA-seq Data Processing and Differential Expressed Gene Analysis. One microgram SDX total RNA from three WT and nine transgenic lines was used for the RNA-seq library construction following the TruSeq RNA Sample Prep v2 LS protocol (Illumina). Six RNA-seq libraries were pooled at equal concentrations for multiplex sequencing. Libraries were assayed for quality and quantity (NCSU Genomic Sciences Laboratory) and sent for sequencing by BGI on an Illumina HiSEq. 2000. The resulting sequences (~100b) were mapped to the *P. trichocarpa* genome v2.0, gene annotation v2.2 (www.phytozome.org) using TOPHAT (23). The frequency of raw counts was determined by BEDtools (24) and normalized using the Trimmed mean of M value (TMM) (25). The genes with a count lower than 15 per million per library were filtered out, and differential expressed genes (DEGs) were obtained by pairwise comparison of transgenic and WT libraries using edgeR/Bioconductor (26). The significance of DEGs is based on a false discovery rate (FDR) of 0.05. We inferred the protein domains in the full *P. trichocarpa* proteome and in the DEGs using InterproScan (27) and estimated the extent of enrichment of specific domains in the DEGs using hypergeometric probability (28).

Laccase Enzyme Assays. Laccase purification and enzyme assay followed Berth et al. (29) with modificaitons. Three grams of SDX was homogenized in 15 mL extraction buffer [25 mM Tris, pH 7.0, 200 mM $CaCl_2$, 10% (vol/vol) glycerol, 4 μM sodium cacodylate, 1 mM PMSF, 1 mg/mL leupeptin, and 1 mg/mL pepstatin A]. Proteins were eluted from Concanavalin-A Sepharose with 10 mL elution buffer (29), and 50 μL was used in the enzyme assays (29).

Construction of a Genetic Regulatory Network using a Graphic Gaussian Model Algorithm. First, we developed and used a graphic Gaussian model (GGM) bottom-up algorithm to calculate relationships of selected genes with specific transcription factors (TFs) selected from a full genomewide pool of TFs. We constructed a three-layer genetic regulatory network (GRN) beginning with those genes that encode enriched protein domains of either laccases (also classified as types 1, 2, and 3 multicopper oxidases), chalcone/stilbene synthases, or peroxidases. Beginning with these genes as the bottom (first layer) of a hierarchical network, we used the GGM to select TFs that represent the next level of regulators in the network (second layer). The selected TFs were then used in the same way to select a higher level of regulators, providing a three-layered GRN. The GGM bottom-up algorithm works as follows. First, it selects a pair of genes, x and y from the bottom layer, and then examines their relationships with each TF from a genomewide TF pool that includes 1,208 TFs and ptr-miR397a. Transcript abundance data were obtained from RNA-seq. Relative abundance of ptr-miR397a was obtained by qRT-PCR. We tested if the interaction with any TF (or ptr-miR397a) denoted as z, increases the correlation of x and y. We calculated Spearman partial correlations between x and y in the absence of z, $r_{xy|z} = pcor(x, y|z)$ and compared this with the x and y correlation, r_{xy}, where r_{xy} is the Spearman coefficient (ρ) of variables x and y. If r_{xy} is significant and $r_{xy|z} = 0$ (insignificant), then z interferes with the correlation of x and y. If r_{xy} is significant and $r_{xy|z}$ is significant, we tested the significance of difference d following (30), where

$$d = r_{xy} - \frac{r_{xy} - r_{zx}r_{zy}}{\sqrt{\left(1 - r_{zx}^2\right)\left(1 - r_{zy}^2\right)}}.$$

If d is significant, we infer that z interferes (regulates) x and y. After all combinations of x and y in the bottom layer were tested with all TFs, we sorted all TF genes based on the total number of times each of them interfered with all pairwise combinations of genes in the bottom layer. TF genes, with high interference frequencies (including ptr-miR397a), were selected to be the second-layer regulators. The same procedure was then applied to the second layer of regulators to obtain the third layers of regulators.

1. Li Q, et al. (2011) Down-regulation of glycosyltransferase 8D genes in *Populus trichocarpa* caused reduced mechanical strength and xylan content in wood. *Tree Physiol* 31(2):226–236.
2. Tuskan GA, et al. (2006) The genome of black cottonwood, *Populus trichocarpa* (Torr. & Gray). *Science* 313(5793):1596–1604.
3. Altschul SF, et al. (1997) Gapped BLAST and PSI-BLAST: A new generation of protein database search programs. *Nucleic Acids Res* 25(17):3389–3402.
4. Ma Y, et al. (2012) Genome-wide identification and characterization of novel genes involved in terpenoid biosynthesis in *Salvia miltiorrhiza*. *J Exp Bot* 63(7):2809–2823.
5. Wu B, et al. (2012) Comprehensive transcriptome analysis reveals novel genes involved in cardiac glycoside biosynthesis and mlncRNAs associated with secondary metabolism and stress response in *Digitalis purpurea*. *BMC Genomics* 13(1):15.
6. Tamura K, et al. (2011) MEGA5: Molecular evolutionary genetics analysis using maximum likelihood, evolutionary distance, and maximum parsimony methods. *Mol Biol Evol* 28(10):2731–2739.
7. Chang S, Puryear J, Cairney J (1993) A simple and efficient method for isolating RNA from pine trees. *Plant Mol Biol Rep* 11(2):113–116.
8. Lu S, Zhou Y, Li L, Chiang VL (2006) Distinct roles of cinnamate 4-hydroxylase genes in Populus. *Plant Cell Physiol* 47(7):905–914.
9. Lu S, Sun YH, Amerson H, Chiang VL (2007) MicroRNAs in loblolly pine (*Pinus taeda* L.) and their association with fusiform rust gall development. *Plant J* 51(6):1077–1098.
10. Dai X, Zhuang Z, Zhao PX (2011) Computational analysis of miRNA targets in plants: Current status and challenges. *Brief Bioinform* 12(2):115–121.
11. Lu S, et al. (2005) Novel and mechanical stress-responsive MicroRNAs in *Populus trichocarpa* that are absent from Arabidopsis. *Plant Cell* 17(8):2186–2203.
12. Song J, Lu S, Chen ZZ, Lourenco R, Chiang VL (2006) Genetic transformation of *Populus trichocarpa* genotype Nisqually-1: A functional genomic tool for woody plants. *Plant Cell Physiol* 47(11):1582–1589.
13. Shi R, Sun YH, Zhang XH, Chiang VL (2012) Poly(T) adaptor RT-PCR. *Methods Mol Biol* 822:53–66.
14. Yeh TF, et al. (2005) Rapid screening of wood chemical component variations using transmittance near-infrared spectroscopy. *J Agric Food Chem* 53(9):3328–3332.
15. Dence CW (1992) The determination of lignin. *Methods in Lignin Chemistry* eds Lin SY, Dence CW (Springer, Berlin Heidelberg), pp 33–61.
16. Blakeney AB, Harris PJ, Henry RJ, Stone BA (1983) A simple and rapid preparation of alditol acetates for monosaccharide analysis. *Carbohydr Res* 113(2):291–299.
17. Bitter T, Muir HM (1962) A modified uronic acid carbazole reaction. *Anal Biochem* 4(4):330–334.
18. Katahira R, Nakatsubo F (2001) Determination of nitrobenzene oxidation products by GC and H-1-NMR spectroscopy using 5-iodovanillin as a new internal standard. *J Wood Sci* 47(5):378–382.
19. Chang H, Cowling EB, Brown W (1975) Comparative studies on cellulolytic enzyme lignin and milled wood lignin of sweetgum and spruce. *Holzforschung* 29(5):153–159.
20. Kim H, Ralph J, Akiyama T (2008) Solution-state 2D NMR of ball-milled plant cell wall gels in DMSO-d(6). *Bioenergy Res* 1(1):56–66.
21. Kim H, Ralph J (2010) Solution-state 2D NMR of ball-milled plant cell wall gels in DMSO-d(6)/pyridine-d(5). *Org Biomol Chem* 8(3):576–591.
22. Kupče E, Freeman R (2007) Compensated adiabatic inversion pulses: broadband INEPT and HSQC. *J Magn Reson* 187(2):258–265.
23. Trapnell C, Pachter L, Salzberg SL (2009) TopHat: Discovering splice junctions with RNA-Seq. *Bioinformatics* 25(9):1105–1111.
24. Quinlan AR, Hall IM (2010) BEDTools: A flexible suite of utilities for comparing genomic features. *Bioinformatics* 26(6):841–842.
25. Robinson MD, Oshlack A (2010) A scaling normalization method for differential expression analysis of RNA-seq data. *Genome Biol* 11(3):R25.
26. Robinson MD, McCarthy DJ, Smyth GK (2010) edgeR: A Bioconductor package for differential expression analysis of digital gene expression data. *Bioinformatics* 26(1): 139–140.
27. Zdobnov EM, Apweiler R (2001) InterProScan: An integration platform for the signature-recognition methods in InterPro. *Bioinf* 17(9):847–848.
28. Wei H, et al. (2013) Global transcriptomic profiling of aspen trees under elevated [CO2] to identify potential molecular mechanisms responsible for enhanced radial growth. *J Plant Res* 126(2):305–320.
29. Berthet S, et al. (2011) Disruption of LACCASE4 and 17 results in tissue-specific alterations to lignification of *Arabidopsis thaliana* stems. *Plant Cell* 23(3):1124–1137.
30. MacKinnon DP, Lockwood CM, Hoffman JM, West SG, Sheets V (2002) A comparison of methods to test mediation and other intervening variable effects. *Psychol Methods* 7(1):83–104.

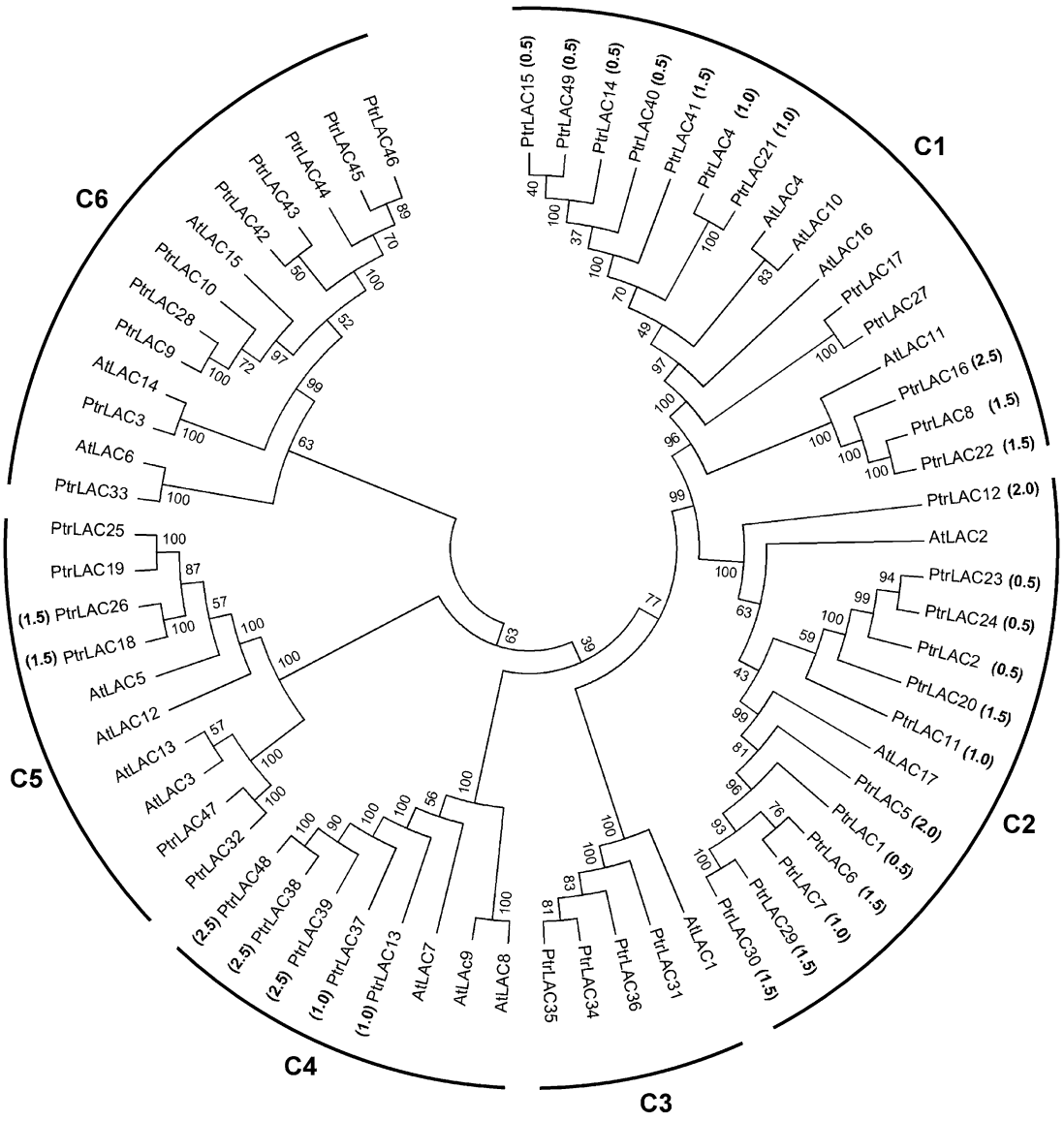

Fig. S1. Phylogenetic relationships of 49 *P. trichocarpa* laccases and 17 *Arabidopsis* laccases. Six clades are indicated by C1–C6. Penalty scores for mismatched patterns in ptr-miR397a:*PtrLAC* duplexes within a 20-base sequence window are shown in parentheses. Among the 17 *PtrLAC*s abundantly expressed in SDX, 13 (*PtrLAC2*, *7*, *11*, *12*, *14*, *15*, *18*, *23*, *24*, *26*, *30*, *40*, and *49*) are targets of ptr-miR397a, whereas the other 4 (*PtrLAC 17*, *19*, *25*, and *27*) are not targets.

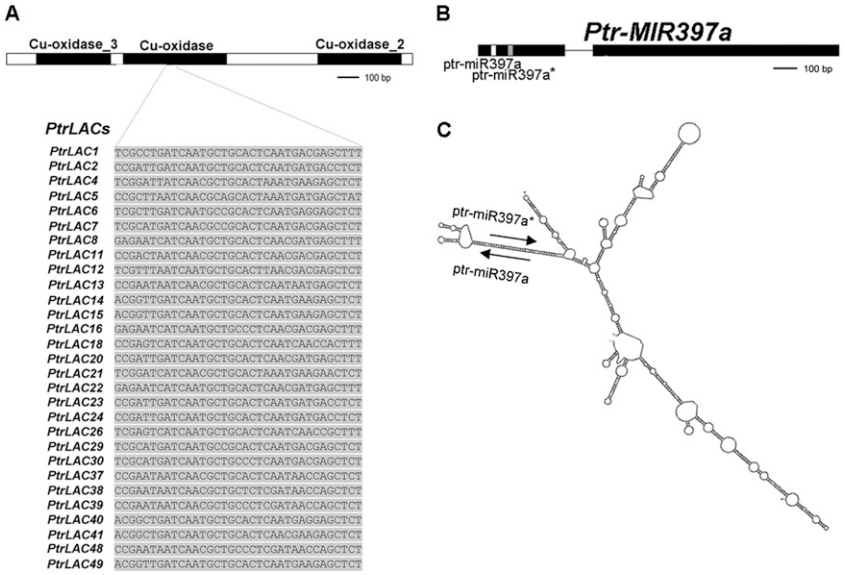

Fig. S2. Ptr-miR397a and its targets. (*A*) Ptr-miR397a targets 29 *PtrLACs* for cleavage. (*B*) *Ptr-MIR397a* gene structure with the location of ptr-miR397a and ptr-miR397a* shown. Black boxes represent exons. A 116-bp intron was found in *Ptr-MIR397a* by aligning the cDNA sequence against the genome sequence (v2.2). (*C*) The predicted secondary structure of the first 800 nucleotides of *Ptr-MIR397a* cDNA. Arrows indicate the orientation of ptr-miR397a and ptr-miR397a*.

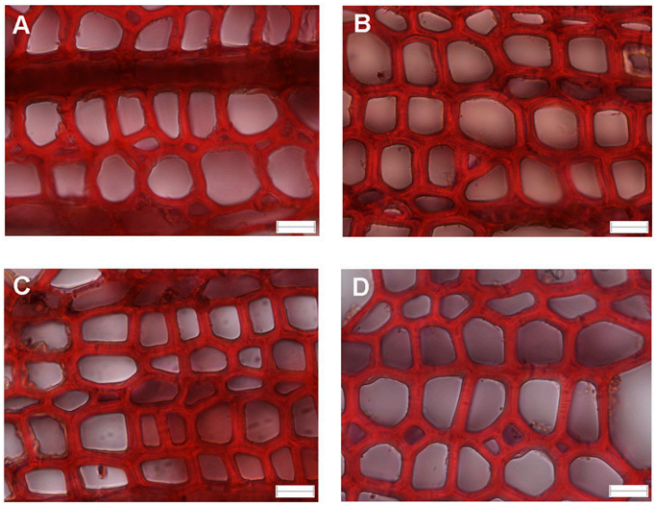

Fig. S3. Comparison of wood anatomical structures between ptr-miR397a transgenic and WT plants. Digital images of transverse stem sections from (*A*) 397-WT1, (*B*) 397-WT2, (*C*) 397-6, and (*D*) 397-10 were taken under a light microscope at ×1,000 magnification. (Scale bars, 10 μm.)

Table S1. Identification of 49 laccase gene models in the *P. trichocarpa* genome

Laccase name	Gene model
PtrLAC1	POPTR_0001s14010
PtrLAC2	POPTR_0001s18500
PtrLAC3	POPTR_0001s21380
PtrLAC4	POPTR_0001s25580
PtrLAC5	POPTR_0001s35740
PtrLAC6	POPTR_0001s41160
PtrLAC7	POPTR_0001s41170
PtrLAC8	POPTR_0004s16370
PtrLAC9	POPTR_0005s22240
PtrLAC10	POPTR_0005s22250
PtrLAC11	POPTR_0006s08740
PtrLAC12	POPTR_0006s08780
PtrLAC13	POPTR_0006s09520
PtrLAC14	POPTR_0006s09830
PtrLAC15	POPTR_0006s09840
PtrLAC16	POPTR_0007s13050
PtrLAC17	POPTR_0008s06430
PtrLAC18	POPTR_0008s07370
PtrLAC19	POPTR_0008s07380
PtrLAC20	POPTR_0009s03940
PtrLAC21	POPTR_0009s04720
PtrLAC22	POPTR_0009s10550
PtrLAC23	POPTR_0009s15840
PtrLAC24	POPTR_0009s15860
PtrLAC25	POPTR_0010s19080
PtrLAC26	POPTR_0010s19090
PtrLAC27	POPTR_0010s20050
PtrLAC28	POPTR_0011s06880
PtrLAC29	POPTR_0011s12090
PtrLAC30	POPTR_0011s12100
PtrLAC31	POPTR_0012s04620
PtrLAC32	POPTR_0013s14890
PtrLAC33	POPTR_0014s09610
PtrLAC34	POPTR_0015s04340
PtrLAC35	POPTR_0015s04350
PtrLAC36	POPTR_0015s04370
PtrLAC37	POPTR_0016s11500
PtrLAC38	POPTR_0016s11520
PtrLAC39	POPTR_0016s11540
PtrLAC40	POPTR_0016s11950
PtrLAC41	POPTR_0016s11960
PtrLAC42	POPTR_0019s11810
PtrLAC43	POPTR_0019s11820
PtrLAC44	POPTR_0019s11830
PtrLAC45	POPTR_0019s11850
PtrLAC46	POPTR_0019s11860
PtrLAC47	POPTR_0019s14530
PtrLAC48	POPTR_0091s00270
PtrLAC49	POPTR_0958s00200

Table S2. NMR-derived H:G:S and interunit linkage data for WT and transgenic lignin samples

Sample	%H	%G	%S	%PB	S/G	%A	%B	%C	%SD
WT1	0.2	32.3	67.5	2.5	2.09	86.5	3.7	7.3	2.4
397-1	0.2	31.3	68.5	2.1	2.19	88.0	3.1	6.6	2.3
397-9	0.3	24.7	74.9	2.9	3.03	89.9	2.3	6.0	1.8
397-10	0.3	28.0	71.8	2.4	2.56	88.5	2.9	6.1	2.6

%PB is based on the total lignin and was not included in the total lignin. A, β–O–4 (β-aryl ether); B, β–5 (phenylcoumaran); C, β–β (resinol); SD, β-1 (spirodienone) (see Figs. 4 and 5 for structures).

Table S3. Effects on transcript abundance of 34 SDX-expressed laccase genes by *Ptr-MIR397a* overexpression

Gene	Read count average in WT SDX	Read count average in transgenic SDX	logFC	logCPM	*P* value	FDR
PtrLAC1	21.49	3.04	−2.85	2.92	<0.001	**<0.001**
PtrLAC2	85.23	14.61	−2.38	5.00	<0.001	**<0.001**
PtrLAC24	243.72	55.57	−1.97	6.68	<0.001	**<0.001**
PtrLAC18	408.64	106.52	−1.91	7.51	<0.001	**<0.001**
PtrLAC23	204.93	61.55	−1.58	6.60	<0.001	**<0.001**
PtrLAC40	148.70	46.44	−1.73	6.17	<0.001	**<0.001**
PtrLAC15	193.96	74.23	−1.40	6.70	<0.001	**<0.001**
PtrLAC26	107.71	42.92	−1.28	5.88	<0.001	**<0.001**
PtrLAC14	159.20	65.55	−1.30	6.47	<0.001	**<0.001**
PtrLAC41	23.78	9.43	−1.42	3.70	<0.001	**<0.001**
PtrLAC49	130.69	54.82	−1.27	6.20	<0.001	**<0.001**
PtrLAC20	30.16	58.18	1.10	5.68	<0.001	**<0.001**
PtrLAC30	51.49	32.79	−0.63	5.23	<0.001	**0.007**
PtrLAC44	26.40	17.20	−0.70	4.29	<0.001	**0.016**
PtrLAC45	22.39	14.56	−0.72	4.05	<0.001	**0.017**
PtrLAC8	5.16	3.25	−0.73	1.92	0.001	**0.030**
PtrLAC25	118.27	179.58	0.69	7.36	0.001	**0.035**
PtrLAC46	17.28	11.54	−0.64	3.70	0.001	**0.039**
PtrLAC43	46.95	32.12	−0.54	5.16	0.001	**0.049**
PtrLAC6	7.17	4.68	−0.56	2.40	0.001	0.053
PtrLAC29	19.64	13.86	−0.54	3.93	0.003	0.113
PtrLAC21	69.36	50.62	−0.43	5.79	0.006	0.164
PtrLAC42	23.67	17.14	−0.46	4.23	0.006	0.168
PtrLAC7	109.19	82.45	−0.38	6.48	0.014	0.261
PtrLAC12	133.44	106.64	−0.33	6.82	0.050	0.515
PtrLAC33	11.33	9.23	−0.25	3.29	0.100	0.707
PtrLAC11	313.90	262.03	−0.31	8.10	0.113	0.735
PtrLAC17	201.96	236.67	0.25	7.83	0.188	0.865
PtrLAC5	8.12	7.01	−0.33	2.87	0.224	0.911
PtrLAC19	185.25	163.46	−0.16	7.40	0.273	0.946
PtrLAC16	21.93	20.51	−0.06	4.38	0.573	1.000
PtrLAC27	266.91	284.15	0.08	8.13	0.609	1.000
PtrLAC4	2.93	2.64	−0.17	1.44	0.483	1.000
PtrLAC47	3.80	3.87	0.08	1.94	0.894	1.000

cpm, read counts per million reads; FC, fold change. FDR value <0.05 is bold.

Table S4. Fifty enriched protein domains identified from 459 DEGS in the context of genomic background

Interpro ID	*P* value	Description	Gene number in DEGs vs. that in the genome
IPR001154	0	DNA topoisomerase II, eukaryotic-type	2:2
IPR017761	5.2375E−26	Laccase	20:34
IPR002355	1.51259E−24	Multicopper oxidase, copper-binding	20:38
IPR001117	9.8465E−22	Multicopper oxidase, type 1	20:48
IPR011706	9.8465E−22	Multicopper oxidase, type 2	20:48
IPR011707	9.8465E−22	Multicopper oxidase, type 3	20:48
IPR008972	4.2319E−17	Cupredoxin	20:74
IPR001099	8.0448E−07	Chalcone/stilbene synthase, N-terminal	4:5
IPR011141	8.0448E−07	Polyketide synthase, type III	4:5
IPR018088	8.0448E−07	Chalcone/stilbene synthase, active site	4:5
IPR001404	2.8492E−06	Heat shock protein Hsp90	5:10
IPR004022	6.1593E−06	DDT family	5:11
IPR018500	6.1593E−06	DDT subgroup	5:11
IPR018501	6.1593E−06	DDT superfamily	5:11
IPR000823	1.03912E−05	Plant peroxidase	7:28
IPR001371	0.000012151	Glycoside hydrolase, family 14B, plant	5:12
IPR011684	0.000012151	KIP1-like	5:12
IPR018238	0.000012151	Glycoside hydrolase, family 14	5:12
IPR001752	2.02377E-05	Kinesin, motor region	11:86
IPR001554	0.00006285	Glycoside hydrolase, family 14	5:15
IPR006766	0.00006285	Phosphate-induced protein 1	5:15
IPR002068	0.000068297	Heat shock protein Hsp20	6:24
IPR010255	0.000211595	Haem peroxidase	7:40
IPR002483	0.000220813	Splicing factor PWI	3:5
IPR016140	0.00111454	Bifunctional inhibitor/plant lipid transfer	6:35
IPR008978	0.00136175	HSP20-like chaperone	6:36
IPR008263	0.00207824	Glycoside hydrolase, family 16	4:15
IPR000167	0.00248467	Dehydrin	2:3
IPR002160	0.00248467	Proteinase inhibitor I3, Kunitz legume	2:3
IPR002205	0.00248467	DNA topoisomerase, type IIA	2:3
IPR011065	0.00248467	Kunitz inhibitor ST1-like	2:3
IPR013757	0.00248467	DNA topoisomerase, type IIA	2:3
IPR013758	0.00248467	DNA topoisomerase, type IIA	2:3
IPR002016	0.00262713	Haem peroxidase, plant/fungal/bacterial	7:55
IPR012328	0.0029749	Chalcone and stilbene synthases	4:16
IPR003594	0.0092599	ATP-binding region, ATPase-like	7:65
IPR001241	0.0098046	DNA topoisomerase, type IIA	2:4
IPR013506	0.0098046	DNA topoisomerase, type IIA	2:4
IPR013759	0.0098046	DNA topoisomerase, type IIA	2:4
IPR015310	0.0098046	Activator of Hsp90 ATPase, N-terminal	2:4
IPR013770	0.0099303	Plant lipid transfer protein	4:20
IPR004648	0.0133661	Tetrapeptide transporter	3:11
IPR016197	0.0197349	Chromo domain-like	3:12
IPR000232	0.0206148	Heat shock factor (HSF)-type, DNA-binding	4:23
IPR010544	0.0241763	Kinesin-related	2:5
IPR013760	0.0241763	DNA topoisomerase, type IIA, central	2:5
IPR018368	0.028073	Chaperonin ClpA/B, conserved site	3:13
IPR013126	0.0315926	Heat shock protein 70	4:25
IPR000109	0.043247923	TGF-beta receptor	5:42
IPR003480	0.046569755	Transferase	4:27

Table S5. Gene models of the genes listed in Fig. 6

Gene name	Gene model
PtrPO2	POPTR_0003s21620
PtrPO3	POPTR_0002s01960
PtrPO6	POPTR_0007s13420
PtrPO34	POPTR_0001s04840
PtrARF2	POPTR_0015s11660
PtrMYB52	POPTR_0007s01430
PtrDAG1	POPTR_0014s09640
PtrUNE12	POPTR_0002s04620
PtrHSFB4	POPTR_0001s28040
PtrMYB50	POPTR_0015s09430
PtrMYB52	POPTR_0007s01430
PtrMYB73	POPTR_0007s10490
PtrNF-YC9	POPTR_0013s02580
PtrABF3	POPTR_0009s10400
PtrARF8	POPTR_0017s01870
PtrARF7	POPTR_0006s07740
PtrMYBCDC5	POPTR_0019s03520
PtrMYB42	POPTR_0003s11360
PtrHB-1–1	POPTR_0011s05660
PtrHB-1	POPTR_0004s04840

Table S6. Primers used for qRT-PCR analysis of laccase gene expression

Gene name	Forward primer	Reverse primer
PtrLAC1	ATTAATGGACTCCCAGGGCCATTA	TTCACATACACAGCATCAGCTTCC
PtrLAC2	AGTTTTGAGTTTCACCAATATTACCTG	CCAGAGGCAGCTCATAGCAAAT
PtrLAC3	TCACCATCAATGGAGAACCAGGATA	GCCAGGGGTGATCATTAGATAGTCT
PtrLAC4	AGGGAGGATATAATTTACCAGTACGG	CAATGGTGTCGATTTTGAAGGGTTTA
PtrLAC5	GGCAAGACTTACATGCTCCGCTTA	AAACAGCATCAACATCAACAATGGTA
PtrLAC6	CTCTGATGCCTACACTATCAATGGAT	TGGTTTCACATAAATAGCATCAACAC
PtrLAC7	CTCTGATGCCTACACTATCAATGGAT	GTTTGCTATGCTGAAGAAGAGCTCG
PtrLAC8	CATACCATTAATGGGAAGCCAGGGA	CAATCAGTACTGCTTGAGTGGTAAAAT
PtrLAC9	CATTCACTGGCATGGAGTGAAACAA	GCCACCATAATGTTCCTTCTTCGTT
PtrLAC10	GAGACACAATCTATGTTACGGTCCAT	CCAGGTTGGATTGGACACTGTGTA
PtrLAC11	GGCCTTCCAGGGCCTTTATACAAT	CTGGACTGATGAGGAGCGTGTCA
PtrLAC12	CCAGGAAAAACCTATCTCCTTCGTT	CGGGGTGATGAGTACAATGTGGGT
PtrLAC13	CTACCCTTGCTCTCAAAACAGAATATT	CGATGACAACAACGCCAGTGACG
PtrLAC14	TGCCTCTTCCCTGCTTTGGTCC	GCCATTGACGGTAACAATCGGC
PtrLAC15	TCTTGCTGTCTGCCTCCTCCCC	GCCATTGACGGTAACAATCGGC
PtrLAC16	CATACTTTTGCAATGGAGATTGAATCA	ATCTGCCTGGAACTTGGTTGGCTA
PtrLAC17	ACCTCCCAGTGACCTCCCCAAC	CTTTGTTTGAGCACTTGAGCCCAG
PtrLAC18	GGTCAACCTGGTGATCTTTTTAACTGC	AACTGTAAACTTGTGGTTGGCTATG
PtrLAC19	CTTGGTAGAGAATGGAGTTGGAC	TTGTCGGGCTTATGAATTCCAAC
PtrLAC20	GCTGATCCTGAGGCAGTGATTAGA	AAGGTTGGTCTCAAAAGGCTTCACA
PtrLAC21	CACGGAGGGTATAATTTATCAGTACAT	CAACGGTGTCGATTTTGAAGGGTTTT
PtrLAC22	ATACATTTACCTTGGAGGTTGAACAG	CAATTAGTATGGTTTGAGTTGTAAAGG
PtrLAC23	CGAGGCACTACAAGTTCAACATAG	CCATTAACAGTCACCATGCTCTTC
PtrLAC24	AGTTTTGAGTTTCACCAATAGTACCTA	CCAGAGGCAGCTCATAGCAAAG
PtrLAC25	CTTGGTCGAGAATGGAGTCGGAG	GCTTATGAATTTCAACAAACTGGTACG
PtrLAC26	GGTCAACCTGGTGATCTTTATAATTGT	TAAGATAAGAGGCATCAGCACCAATA
PtrLAC27	ATGAGTCAATACTACCACCTCCT	CTATACTCCTCCCTCCCGCATC
PtrLAC28	CACAAGACTCTGCAGCACCAAGAA	GGCTGTTTCACTCCATGCCAGTGA
PtrLAC29	AGGCCCAAATGTCTCTGATGCTTAT	AAGAAGAGCTCGTCATTGAGTGCG
PtrLAC30	GCAGATCCAGAGGCGATCATTAGT	AAGAAGAGCTCGTCATTGAGGGCA
PtrLAC31	ATGCCGTATCCATTCTCAGCTCAG	GGCATTCCATTTATGGTGTAAGCGT
PtrLAC32	GTAATCTTCAGTTTCCAAGCTCATTT	TTTGATCACAAGAGTATCGCCATCG
PtrLAC33	GGCACCTTCTTCTGGCATGCTCAT	AGATGTACAATATCCTGAAGCCAGTA
PtrLAC34	GGCGTTACCGTGTTGTTCTTCAC	CAATCCGATTTTTGACCTTAATATGAATAC
PtrLAC35	ACGAAGCAGCTTCTAATGGTGAAC	TCTGAGCAATCCGATTTTTGACC
PtrLAC36	GGGATCCAGATGAAGTTGAAAACAG	GCTATCGCAAAGAAGAGCTCATCC
PtrLAC37	TGTTGATGTCGAAAACCAGGCAGAA	GATTGGCTATCTTGAAAAAGAGCTGG
PtrLAC38	GCTTCTGCTGCAATTGTGGAACG	AAGCGTTGGGCCTGGCAAGCTG
PtrLAC39	GATCCTGTCAACGACCATAAGAAT	CCAGATGACAGTGAAAGAACCAC
PtrLAC40	AAGGCGGTTTCACTTTGCCAGTCC	TAGGTGGCATCAACTTCCACGACA
PtrLAC41	GGGCGGTTTCACATTGCCAGTCG	GTAGGTGGCATCAACTTCCACAAG
PtrLAC42	ACAATTATTATTGGATCTTGGTTTAAGG	CATTGATGGTAAGACTGTTGGATATATT
PtrLAC43	GAAATCAACACTGTTGCACTTCG	GGCGCATACTTTGTGCCGTTGTAT
PtrLAC44	ACAATTATTATTGGATCTTGGTTTAAGG	CATTGATGGTAAGACTGTTGGATATATT
PtrLAC45	ACAATTATTATTGGATCTTGGTTTAAGC	CCATTGATGGTAAGACTATTGGATGG
PtrLAC46	GCAACTGGTGCTGGACCTGCAAT	TTAACCTTCAAACGGTATGTGTTTTCT
PtrLAC47	GTAATCATCAGTTTCCAAGCATCTTC	CTTGATCACAAGAGTATCACCGTCA
PtrLAC48	GCTCATTCTATGTGAAAAACCTTACAG	AGCGTTGGGCCTGGCAAGCTT
PtrLAC49	CAGCAAATATGGAGTACTCCAATTG	TGCCGAATCCTGCACTCGACC
Ptr18SrRNA	CGAAGACGATCAGATACCGTCCTA	TTTCTCATAAGGTGCTGGCGGAGT

Table S7. Primers used for validation of ptr-miR397a targets

Gene name	Gene-specific primer	Nested gene-specific primer
PtrLAC1	ACGTAAGGTCTAGCAGTCATGAAAAATT	GTGGTGGGGTTTGGTCTTGAGAAGG
PtrLAC2	GGCAATGGGTTTGGTCTTCAGAAGAAC	GTGGTCTGTCCTGCTGTTATAACCAAG
PtrLAC13	TGTAATAAGATCCCACTTCCTGGTCT	CGATGACAACAACGCCAGTGACG
PtrLAC18	CTGCCATGTAATATCGGCCAGGTAGT	CTGTGGTTTGGCCAGGTCCTAGCATG
PtrLAC21	CCACGGTTTGCCGTCACAAGAACGTTT	CAACGGTGTCGATTTTGAAGGGTTTT
PtrLAC26	CTGCCATGTAATATCGGCCAGGTAGT	CAGTGGTTTGGCCTGGTCCTAGCATT
PtrLAC30	AGTCGGGTTTGGTTTTCAGAAGAACA	GGTTTGTCCAGGGGTAATGAGAAGT